Scientific Research Publishing

Journal of Transportation Technologies, 2023, 13, 369-388
https://www.scirp.org/journal/jtts
ISSN Online: 2160-0481
ISSN Print: 2160-0473

Simulations of Electric Vehicle Driving Range and Battery Aging Using Experimental Data

Yiqun Liu

College of Engineering Technology, Ferris State University, Big Rapids, USA
Email: YiqunLiu@ferris.edu

How to cite this paper: Liu, Y.Q. (2023) Simulations of Electric Vehicle Driving Range and Battery Aging Using Experimental Data. *Journal of Transportation Technologies*, **13**, 369-388.
https://doi.org/10.4236/jtts.2023.133018

Received: June 6, 2023
Accepted: July 9, 2023
Published: July 12, 2023

Abstract

Driving range and battery aging, which are two important topics considered by consumers when purchasing an electric vehicle, are studied in this research. This research started with experiments on $LiNiMnCoO_2$ battery cells. Experimental results of discharging voltage, OCV, and internal resistance are obtained under different ambient temperatures. Cycle aging of battery cells is also investigated by experiments. The obtained experimental data is used to develop the battery pack model in the electric vehicle model as well as the battery aging model. The developed electric vehicle model is used to investigate electric vehicle's driving range. Within the ambient temperature range between −30˚C to 50˚C, the driving range decreases with the ambient temperature. The driving range can also be heavily reduced by high-speed and aggressive driving. By using the developed battery aging model, cycle aging of the onboard battery of an electric vehicle after its 15,000-hour usage is investigated. Simulation results show that battery cell has a quicker cycle aging process under higher ambient temperatures. Large discharging and charging currents involved in aggressive driving can also accelerate battery aging. In addition, cycle aging of the onboard battery will be accelerated if the battery is almost used up before recharging every time. This research presents a novel approach to studying the driving range and battery aging of electric vehicles and includes valuable results for automotive engineers and consumers of electric vehicles.

Keywords

Lithium-Ion Battery, Battery State Estimation, Powertrain Electrification

1. Introduction

Lithium-ion battery is currently the major type of electrical energy storage device of electrified vehicles because of its high energy density and power density

[1] [2]. However, the performance of lithium-ion battery, including discharging power and usable capacity, changes under different operating temperatures and through battery life. The discharging power and usable capacity of the battery decrease with battery operating temperature. Also, performance of lithium-ion battery degrades through battery life, which includes battery usable capacity decrease and battery impedance increase [3]. The performance degradation through battery life is battery aging. For electrified vehicles, onboard battery packs with smaller usable capacity, lower discharging power, and increased battery impedance make the electric driving range shorter and acceleration less powerful. In addition, an electrified vehicle with a significantly aged battery pack requires battery service or even battery replacement which will tremendously increase the operational cost of the vehicle [4].

The operating temperature of a battery is the combined result of the heat generated by the battery itself and the heat of the ambient environment. Usually, most lithium-ion batteries have a designed acceptable operating temperature range between −20˚C and 60˚C [5]. However, the optimal temperature range is between 15˚C to 35˚C, which is also the comfortable temperature range for humans [6]. With low operating temperatures, chemical reaction and charge transfer in lithium-ion batteries are slower, which results in reduced electrode lithium-ion diffusivity and electrolyte ionic conductivity [7] [8]. The reduced diffusivity and conductivity will lead to decrease of battery's power and energy, or even battery failure. On the other hand, high operating temperatures accelerate battery aging. Lithium-ion and active materials are reduced under high operating temperatures [9]. If high temperature is out of control, self-ignition and even explosion caused by thermal runaway may be triggered.

To determine the battery aging level, state-of-health (SOH) which is usually defined as the percentage of current capacity of the battery compared to its original capacity when the battery was new, is frequently used. A battery is considered at its end-of-life (EOL) if it has a SOH of 80% or lower [10]. Degradation of battery is caused by the effects of either calendar aging or cycle aging or combined [11]. Calendar aging refers to degradation of the battery during its storage. Calendar aging is heavily affected by the storage temperature. Under high storage temperatures, corrosion and lithium loss of lithium-ion batteries are accelerated, which results in shrinkage of battery capacity [12]. Calendar aging is also heavily affected by the state-of-charge (SOC) of the battery during its storage. Before storage, lithium-ion battery should be charged to an optimal SOC level to prolong the battery life [13]. Cycle aging of the battery refers to the degradation of the battery during its utilization. Like calendar aging, cycle aging is also faster under elevated ambient temperature. In addition to that, batteries with a larger variation of SOC in each cycle have a faster cycle aging [14]. Large charging and discharging currents also cause degradation of power and capacity of the battery by accelerating Solid Electrolyte Interphase (SEI) formation on battery electrodes [15] [16]. Lastly, over-charging and over-discharging beyond battery vol-

tage limit can also significantly reduce the life of lithium-ion battery [17] [18] [19].

In this article, driving range and onboard battery cycle aging of an electric vehicle are investigated. First, extensive battery tests are conducted on Lithium-Nickel-Manganese-Cobalt-Oxide battery cells under different operating conditions. Experimental data of discharging voltage vs. depth-of-discharge (DOD), open-circuit voltage (OCV) vs. DOD, internal resistance vs. DOD under different ambient temperatures are obtained. Shrinkage of battery capacity and increase of internal resistance caused by cycle aging are also investigated by experiments. The obtained experimental data is used to develop and calibrate the battery pack model in the electric vehicle model (in AVL-Cruise) as well as the battery aging model (in MATLAB/Simulink). The developed electric vehicle model is used to study the driving range of the electric vehicle, while the developed battery aging model is used to study the cycle aging of the onboard battery of electric vehicle. To the best of author's knowledge, this research is the only one which investigates electric vehicle driving range and battery aging based on first-hand experimental battery data. This manuscript demonstrates a novel and reliable approach to studying the properties of electric vehicles.

The rest of this article is organized as follows: Section 2 presents the experimental setup of battery testing and the obtained experimental results; Section 3 is about the electric vehicle model developed in AVL-Cruise and investigation of electric vehicle driving range; Section 4 is about the battery cell aging model developed in MATLAB/Simulink and the cycle aging simulation of the electric vehicle battery; Section 5 is discussion and conclusion of this research.

2. Battery Cell Testing and Experimental Results

Extensive experiments are conducted on the battery cell to obtain the essential battery characteristics for developing the battery cell simulation models. Battery cells used for testing are EiG ePLB-C020 lithium-ion polymer battery cells. Their cathodes are Lithium-Nickel-Manganese-Cobalt-Oxide ($LiNiMnCoO_2$) based and anodes are graphite based. The detailed specifications of the battery cell [20] are listed in **Table 1**. Battery cell in the test is connected to the Digatron Charge and Discharge Unit (cycler) which can charge and discharge the battery cell using any specified constant current or changing current. The charging and discharging steps can be repeated for any number of cycles. The cycler control software monitors and records testing data, such as charging and discharging power, cell terminal voltage, and energy charged into or discharged from the battery cell. During the tests, battery cells are placed in the temperature chamber which provides a safe controlled testing environment with different specified interior temperatures (ambient temperatures for the battery cell in the test). The experimental setup of the battery testing is shown in **Figure 1**.

All the battery cells used in this research are brand new. Initial testing is performed to ensure battery cells are in good condition. First, each battery cell is

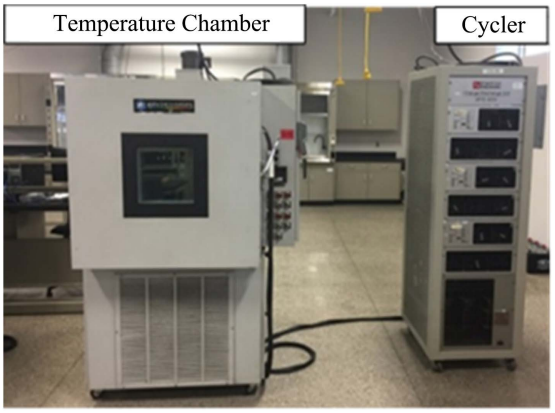

(a)

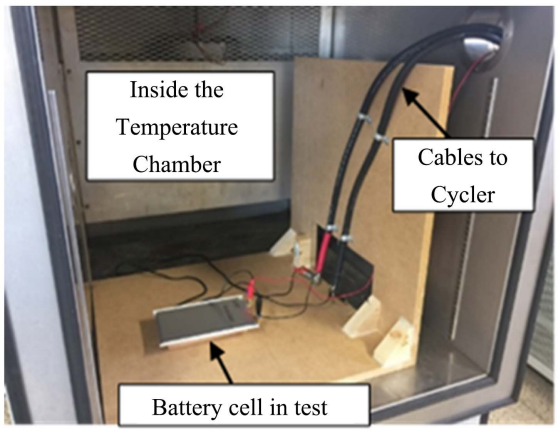

(b)

Figure 1. Experimental setup of the battery testing: (a) Cycler and temperature chamber; (b) Battery cell testing inside the temperature chamber.

Table 1. Specifications of EiG ePLB-C020 battery cell [20].

Length	196 mm
Width	127 mm
Thickness	7 mm
Weight	428 g
Nominal voltage	3.6 V
Nominal capacity	20 Ah
AC impedance (1 kHz)	<3 mΩ
Specific energy	174 Wh/kg
Energy density	370 Wh/L
Specific power (50% DOD, 10 seconds)	2300 W/kg
Power density (50% DOD, 10 seconds)	4600 W/L
Maximum charging voltage	4.15 V
Lower voltage limit for discharge	2.5 V

charged to the maximum charging voltage 4.15 V by constant 1 C rate (20 A) current. After reaching 4.15 V, the cycler gradually reduces the charging current from 20 A to 2 A to keep the charging voltage at 4.15 V. This method is called control voltage charging which can be used to ensure full charge. Then, the battery cell is discharged to the lower voltage limit for discharge, which is 2.5 V, by constant 1 C rate discharging current. After reaching 2.5 V, control voltage discharging is performed to ensure a full discharge. Only battery cells with a full discharging capacity higher than the nominal value (20 Ah) are selected for experiments in this research.

2.1. Ambient Temperature Effects on Battery Cell

After the battery cells for this research are selected, the first test is constant 20 A continuous discharge under different ambient temperatures. The fully charged battery cell is connected to the cycler, then the battery cell is discharged to the lower voltage limit for discharge which is 2.5 V. Before the discharge test starts, the fully charged battery cell is considered to have a DOD of 0%. When the discharging voltage of the battery cell reaches 2.5 V at the end of discharge test, the battery cell is considered to have a DOD of 100%. The discharge tests are performed under four different ambient temperatures, which are −25˚C, 0˚C, 25˚C, and 50˚C. The discharging voltages vs. DOD under different ambient temperatures are plotted in **Figure 2(a)**. The OCVs vs. DOD of the battery cell under different ambient temperatures are also plotted in **Figure 2(a)**. To obtain the OCV vs. DOD, the method called pulse discharge [21] with a resolution of 5% DOD is applied. In each discharging pulse, 5% of the nominal capacity of the battery cell is discharged by a constant 20 A discharging current. There is a 3-minute rest time between each two discharging pulses. During this 3-minute, the battery cell is relaxed without any current flow through. At the end of each 3-minute rest time, the battery cell terminal voltage is measured. These measured cell terminal voltages are the OCVs at the corresponding DOD levels. Blue line in **Figure 2(b)** shows the battery cell terminal voltage during the entire pulse discharge test under 25˚C. The orange dots are the OCV obtained at the end of each 3-minute rest time. The first and last two pulses are not shown in **Figure 2(b)**, so the first and last orange dots represent OCV at 10% DOD and 90% DOD, respectively. The pulse discharge tests are repeated under −25˚C, 0˚C, 25˚C, and 50˚C to obtain the relationship between OCV and DOD under these ambient temperatures.

Figure 2(a) shows that ambient temperature significantly affects the discharging voltage of the battery cell. With the ambient temperature reduces from 50˚C to −25˚C, the discharging voltage at a given DOD level also decreases. It can be seen that the discharging voltage of the battery cell is more sensitive to low ambient temperatures, because the discharging voltage can be reduced by up to 0.5 V when the ambient temperature changes from 0˚C to −25˚C. In addition, **Figure 2(a)** shows that the ambient temperature also has a similar but much

smaller effect on OCV of the battery cell. The voltage difference between the OCV and the discharging voltage of the battery cell under each ambient temperature is the voltage drop caused by the battery cell's internal resistance. The internal resistance can be calculated by dividing the voltage drop by the continuous constant discharging current 20 A. Figure 3 shows the variations in the internal resistance of the battery cell under different ambient temperatures. It shows that the internal resistance is higher under lower ambient temperature and is lower under higher ambient temperature. The internal resistance of the battery cell under −25˚C is more than seven times higher than that under 50˚C. Under ambient temperatures of 0˚C, 25˚C, and 50˚C, internal resistance does not change much over the DOD range between 10% to 80%. However, under −25˚C, the internal resistance is significantly higher when the battery cell is close to fully charged and fully discharged.

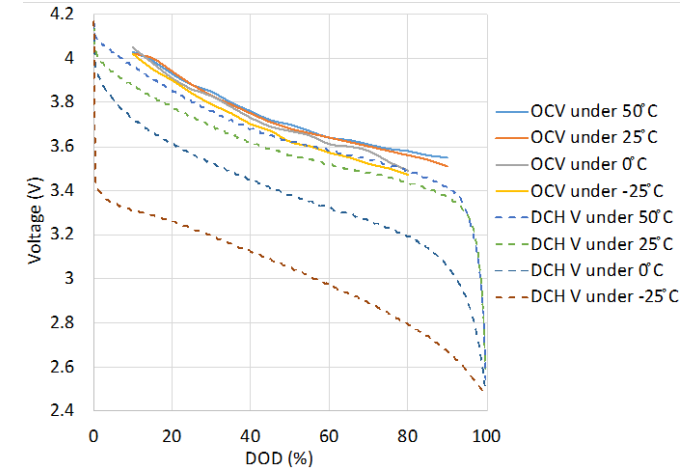

(a)

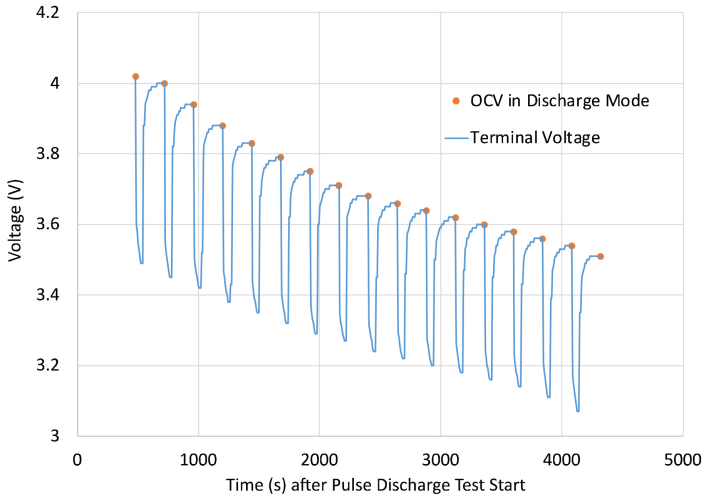

(b)

Figure 2. Experimental voltage data of the battery cell: (a) OCV and discharging voltage (DCH V) of the battery cell under different ambient temperatures; (b) Battery cell terminal voltage and OCV during pulse discharge test under 25˚C.

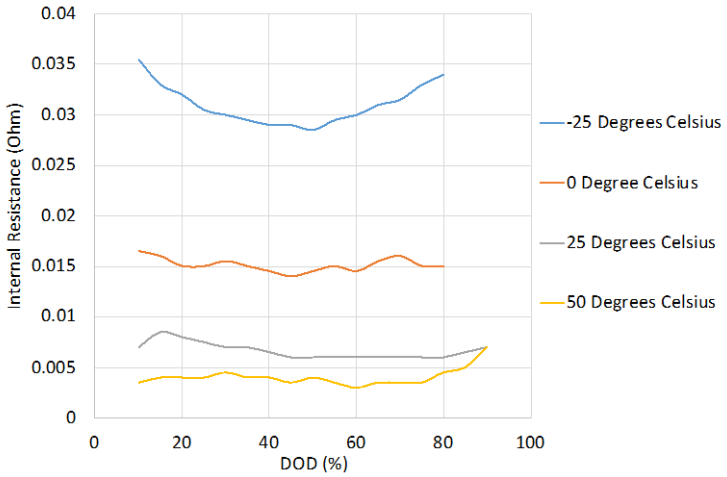

Figure 3. Variations of internal resistance of the battery cell under different ambient temperatures.

2.2. Aging Effects on Battery Cell

Next experiment on the battery cell is the battery aging test. As preparation, the fully charged battery cell is discharged by constant 1 C rate (20 A) discharging current for half an hour, so the battery cell has a 50% DOD with an OCV of about 3.6 V. Then, this cell is charged to 4.15 V, which is the maximum charging voltage of the battery cell. Once the charging voltage increases to 4.15 V, the 40 A discharging step immediately starts and continues until the discharging voltage decreases to 2.15 V, the lower voltage limit of this battery cell. The cycle which combines above 20 A charging and 40 A discharging steps are repeated 800 times. To accelerate the aging process, the 800-cycle aging test is conducted under a higher ambient temperature, which is 35˚C. The 1 C rate discharging voltage and OCV are obtained using the aforementioned methods at the beginning and at the end of the 800 aging cycles. Also, the aging test is interrupted at 200th, 400th, and 600th aging cycle to obtain the 1 C rate discharging voltage and OCV. To resume the aging test after each interruption, preparation steps same as those at the beginning of the aging test are performed.

Figure 4 shows the variation of the discharged energy from each 40 A discharging step of the 800-cycle aging test. Because control voltage charging and discharging are not used in these 800 aging cycles, the discharged energy in each discharging step is smaller than the nominal capacity 20 Ah, even when the battery was brand new. During these 800 aging cycles, the discharging energy in each discharging step reduces from 18 Ah to 13.5 Ah. During the first 50 cycles, the discharged energy in each discharging step has almost no change. After first 50 cycles, the discharged energy in each discharging step starts to reduce gradually, and the decreasing rate becomes faster and faster. From 200th cycle to 600th cycle, the decreasing rate of the discharged energy seems to be constant. After 600th cycle, the discharged energy in each discharging step starts to decrease faster again. **Figure 4** clearly shows that the usable capacity of the battery cell is shrinking during the 800-cycle aging test.

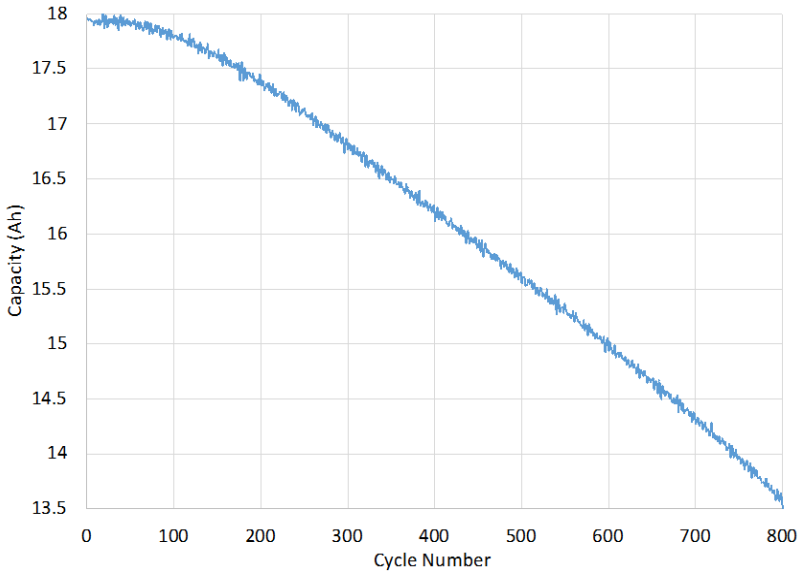

Figure 4. The discharged energy in each discharging step during the 800-cycle aging test.

Figure 5(a) shows the OCV and 1 C rate discharging voltage of the battery cell as a function of DOD when the battery cell was new and after 200th, 400th, 600th, and 800th aging cycle. Battery aging has almost no effect on OCV as the OCV curves overlap with each other. However, battery aging does have significant effect on the discharging voltage. As the battery cell ages, its discharging voltage decreases. At 50% DOD, the 1 C rate discharging voltage of the battery cell after 800 aging cycles is about 0.3 V lower than that of the battery cell when it was brand new. When the battery cell is approaching empty (100% DOD), the above voltage difference is almost 0.6 V. **Figure 5(b)** shows the internal resistance of the battery cell at different aging cycles calculated from the OCV and discharging voltage shown in **Figure 5(a)**. **Figure 5(b)** clearly shows that internal resistance increases with the battery cell ages. After 800 aging cycles, the internal resistance of the battery cell is 3 - 7 times higher than that of the battery cell when it was brand new. Also, for an aged battery cell (after 600 aging cycles), the internal resistance significantly increases when the battery cell is approaching empty.

3. Battery Electric Vehicle Model and Driving Range Simulation

After OCV vs. DOD and internal resistance vs. DOD of the battery cell are obtained, the experimental data is used to develop the battery pack model inside an electric vehicle model in AVL-Cruise. The electric vehicle model is developed based on 2018 Nissan Leaf for two reasons: first, the detailed vehicle specifications of 2018 Nissan Leaf are obtainable; second, 2018 Nissan Leaf uses the same type of battery cell as the battery cell tested in Section 2, which is $LiNiMnCoO_2$. **Table 2** summarizes the specifications of 2018 Nissan Leaf [22], which are used for developing the electric vehicle model in AVL-Cruise. The battery cell tested

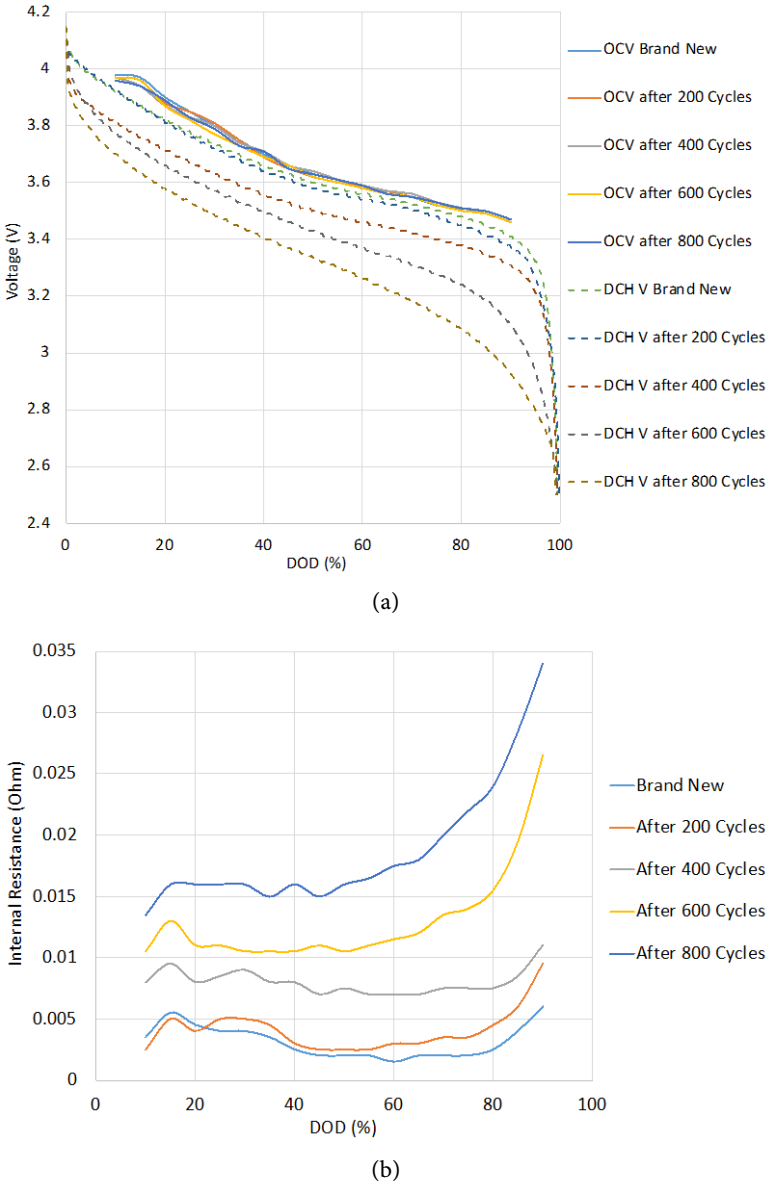

Figure 5. (a) OCV and 1 C rate discharging voltage (DCH V) of the battery cell at different aging cycles; (b) Internal resistance of the battery cell at different aging cycles.

in Section 2 has a nominal voltage of 3.6 V and a nominal capacity of 20 Ah. The battery pack of 2018 Nissan Leaf has 350 V nominal voltage and 40 kWh nominal capacity. To make the developed battery pack model inside the electric vehicle model has a nominal voltage and a nominal capacity close enough to those of the real battery pack of 2018 Nissan Leaf, 100 identical battery cell models are connected in series to form a string and six of these strings are connected in parallel to form the battery pack model. Because each battery cell model uses the obtained OCV vs. DOD and internal resistance vs. DOD experimental data and has a 3.6 V nominal voltage and a 20 Ah nominal capacity, the developed battery pack model with the above connection has nominal voltage of 360 V and nominal capacity of 43.2 kWh. To make the nominal capacity of the battery pack

Table 2. Specifications of 2018 Nissan Leaf [22].

Drivetrain	Front-wheel-drive
Overall length	4490 mm
Overall width	1788 mm
Overall height	1540 mm
Curb weight	1580 Kg
Tire size	215/50 R17
Battery type	$LiNiMnCoO_2$
Battery voltage	350 V
Battery capacity	40 kWh
Electric motor type	AC Synchronous
Max. electric motor power	150 hp/3283 – 9795 rpm
Max. electric motor torque	320 Nm/0 – 3283 rpm

model has the same capacity as the real Nissan Leaf battery pack, which is 40 kWh, the lower capacity limit of the developed battery pack model is set to 7.4%. The developed electric vehicle model in AVL-Cruise is shown in **Figure 6**.

Four standard driving cycles, which are UDDS, WLTP, HWFET, and US06, are used in the simulations. UDDS is a city driving cycle that simulates the urban driving with frequent stops, while HWFET is a higher-speed driving cycle which simulates the highway driving. WLTP driving cycle includes a wide range of driving conditions, which are urban, suburban, main road, and highway. The US06 driving cycle is an aggressive driving cycle that involves many rapid accelerations and decelerations. The vehicle velocity profile combined with the on-board battery pack terminal current profile of the developed electric vehicle model for each driving cycle simulation is shown in **Figure 7**. Positive currents are discharging currents for vehicle propulsion, while negative currents are charging currents during electric vehicle regenerative braking and energy recuperation.

To perform the maximum driving range simulation, the initial SOC of the battery pack of the electric vehicle model is set to 100%, then the electric vehicle model repeats running the same driving cycle under 25˚C ambient temperature until the battery pack SOC reduces to 0%. **Figure 8** shows the simulated battery pack SOC as a function of distance driven. SOCs of the battery pack decrease with the distances driven increase, and the SOCs have relatively linear decrease. The total distance driven at 0% SOC is the maximum driving range for each of these four driving cycle simulations. From **Figure 7**, it can be seen that total area under current curve (which is the total energy consumption) is the smallest for UDDS driving cycle, plus that the frequent deceleration-to-stops enable the regenerative braking to recover the kinetic energy and convert it to electrical energy, that is the reason why UDDS driving cycle gives the electric vehicle the

longest driving range. On the other hand, US06 which is an aggressive driving cycle gives the electric vehicle the shortest driving range because the electrical energy consumption is much higher during US06 cycle.

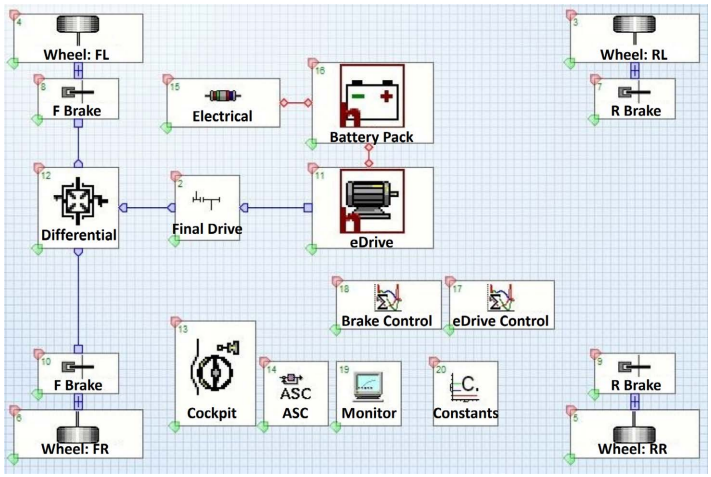

Figure 6. Electric vehicle model based on 2018 Nissan Leaf built in AVL-Cruise.

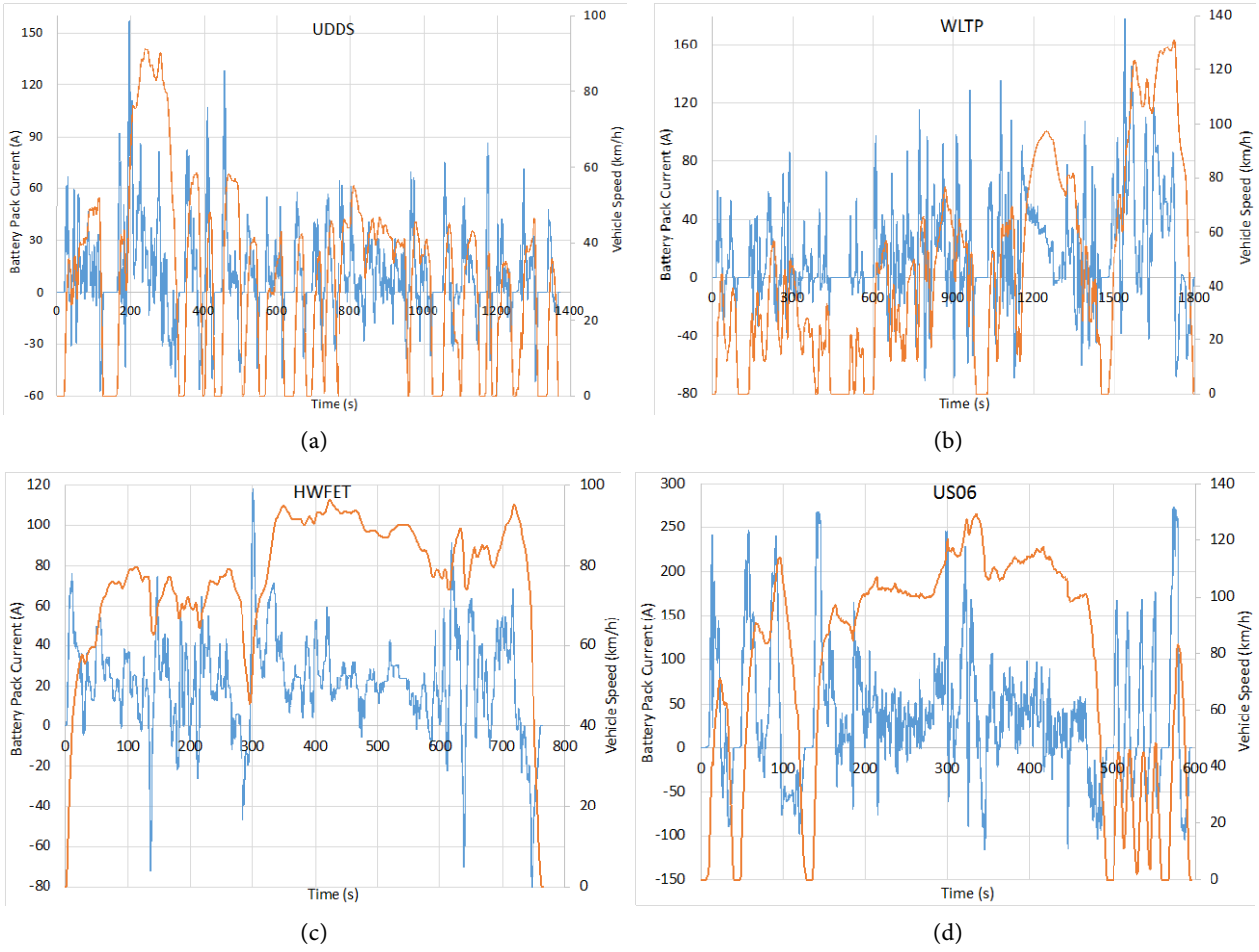

Figure 7. Vehicle speed (orange line) and simulated battery pack terminal current (blue line) during four different driving cycles: (a) UDDS; (b) WLTP; (c) HWFET; (d) US06.

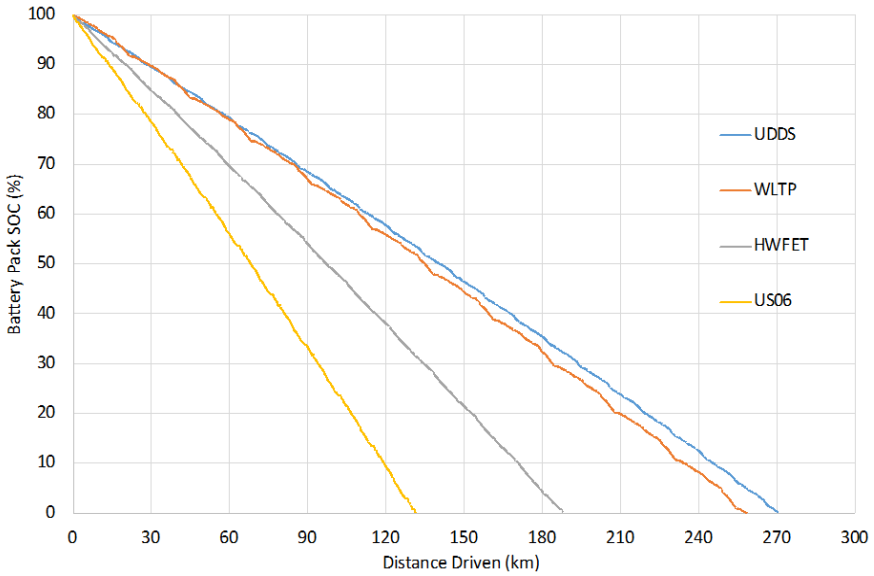

Figure 8. Battery pack SOC decreases with the increase of the distance driven of the electric vehicle under different driving cycle repetitions.

To validate this developed 2018 Nissan Leaf electric vehicle model, the model simulated driving ranges during above four driving cycles are compared with experimental data obtained by AAA [23] and Nissan [22], as shown in **Table 3**. The positive "difference" means that the model simulated driving range is higher than the tested data, and the negative "difference" means that the model simulated driving range is lower than the tested data. The discrepancies are smaller than 5% for WLTP, HWFET, and US06 driving range simulations, and the overall average of all four discrepancies is only 5.42%. The low discrepancy validates that this developed Nissan Leaf electric vehicle model is relatively accurate.

The maximum driving range of electric vehicles is heavily affected by the ambient temperature because the temperature affects on battery internal resistance. To investigate the ambient temperature effects on maximum driving range, nine ambient temperatures which cover the common operating temperature range for electric vehicles are selected. These nine temperatures are −30˚C, −20˚C, −10˚C, 0˚C, 10˚C, 20˚C, 30˚C, 40˚C, and 50˚C. For each ambient temperature, the electric vehicle model repeats the same driving cycles until the battery pack SOC reduces from 100% to 0%. The total distance driven during each simulation is summarized and presented in **Figure 9**. It is clearly seen that driving range reduces with ambient temperature decreases over the entire −30˚C to 50˚C range. With the ambient temperature going down, the decreasing rate of the maximum driving range becomes faster and faster. For ambient temperature below −10˚C, the maximum driving range decreasing rate is about 1.8 km/˚C. At −30˚C, the driving range shrinks about 30% compared to that at 25˚C. Under each selected ambient temperature, UDDS and WLTP driving cycles always result in the longest driving range, and US06 driving cycle always results in the shortest driving range.

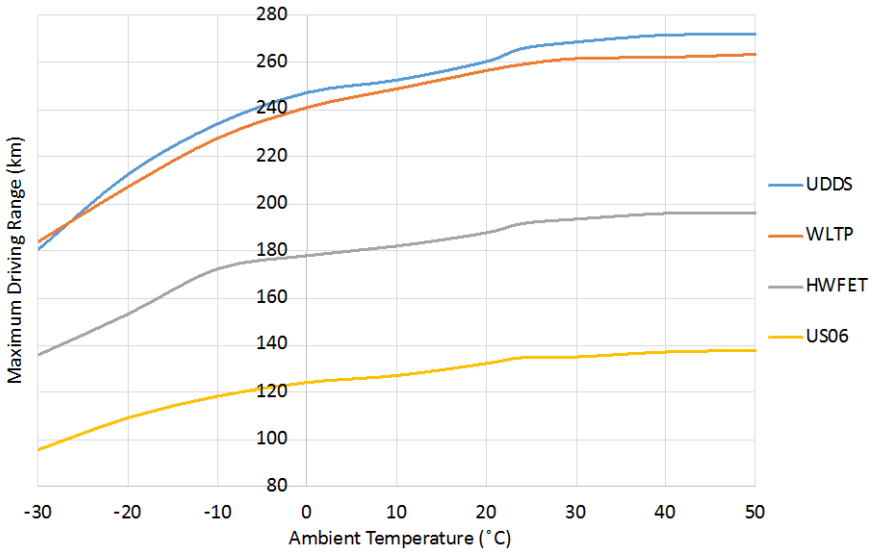

Figure 9. Simulated maximum driving range of the electric vehicle model under different ambient temperatures and different driving cycles.

Table 3. Comparison between model simulated maximum driving range and the tested driving range of 2018 Nissan Leaf under different driving cycles. Tested driving ranges under UDDS, HWFET, and US06 cycles are from AAA [23]. Tested driving range under WLTP cycle is from Nissan [22].

	UDDS	WLTP	HWFET	US06
Simulated Range	266.0 km	259.3 km	191.7 km	134.7 km
Tested Range	244.6 km	270.4 km	199.6 km	141.6 km
Difference	21.4 km	−11.1 km	−7.9 km	−6.9 km
Discrepancy	8.75%	4.11%	3.96%	4.87%

4. Battery Aging Model and Electric Vehicle Battery Aging Simulation

In this section, cycle aging of the onboard battery of an electric vehicle during 10-year usage is investigated by model simulation. A battery aging simulation model is developed in MATLAB/Simulink, as shown in **Figure 10**. In this model, three inputs, which are DOD, battery cell terminal current during driving cycle, and recharge current, are used to generate the repetition. The battery cell terminal current during driving cycle is from the Nissan Leaf model developed in last Section. Because the battery pack in the Nissan Leaf model has six strings in parallel and each string has 100 cells in series, the cell terminal current is 1/6 of the battery pack terminal current. In other words, the simulated battery pack terminal currents presented in **Figure 7** should be divided by six and then be used as the "battery cell terminal current during driving cycle" model input. Another model input is the ambient temperature in ˚C and it is a direct input of the battery cell block. The main output of this model is the remaining usable capacity of the battery cell in Ah. To finish the setup of the battery cell block,

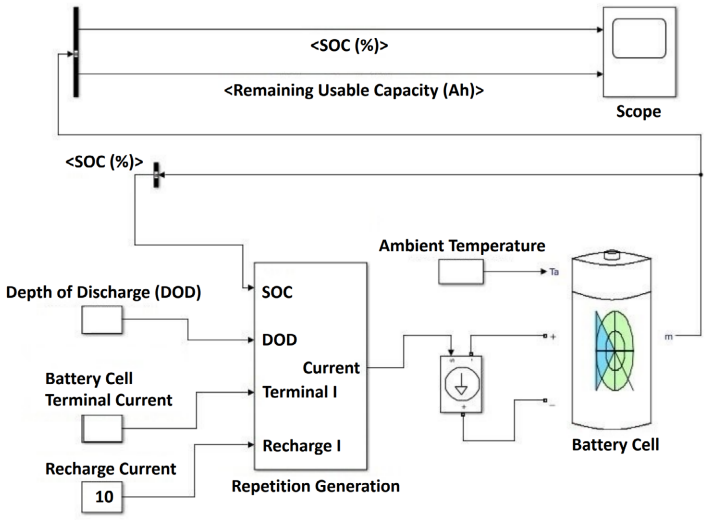

Figure 10. Cycle aging simulation model of battery cell developed in MATLAB/Simulink.

discharging voltage curves and internal resistance curves under different ambient temperatures shown in Figure 2 and Figure 3 are used to calibrate the battery cell block. In addition, experimental battery cell capacities and internal resistances at its beginning of life and end of life are used to enable the cycle aging simulation feature of the battery cell block.

Two investigations of electric vehicle battery cell cycle aging are performed. The first one is to investigate the effects of different ambient temperatures and different driving cycles on battery cell cycle aging. The second one is to investigate the effects of different DOD levels and different driving cycles on battery cell cycle aging. The total simulated duration is set to 15,000 hours. Because if the electric vehicle is assumed to be driven for three hours and to be charged for two hours daily, and the vehicle is used for 300 days per year, 15,000 hours is equivalent to the total number of hours during the 10-year usage of the vehicle.

The simulation results of the first study are shown in Table 4. In this study, the effects of different ambient temperatures and different driving cycles on onboard battery cell cycle aging are investigated. Four ambient temperatures, which are −25˚C, 0˚C, 25˚C, and 50˚C, are selected. For each ambient temperature, four different driving cycles (WLTP, UDDS, HWFET, and US06) are used. In this study, each driving cycle is repeated until the DOD of the battery cell reaches 90%, then the battery cell is fully charged by 10 A current. After the battery cell is fully charged, the repetition of the driving cycle continues. The above steps are repeated for 15,000 simulated hours. Table 4 shows that the original capacity when battery cell was new is smaller under lower ambient temperatures. After 15,000 hours of usage, the usable capacity shrinks between 2.1 Ah to 5 Ah, depending on the ambient temperature and driving cycle. With ambient temperature increases from −25˚C to 50˚C, the shrinkage of usable capacity becomes larger, which means that the battery cell has a quicker cycle aging process under higher operating temperatures. Table 4 also shows that, under the same ambient temperature, the onboard battery cell has larger usable capacity shrin-

kage if the electric vehicle is kept running US06 driving cycle. It means that the large charging and discharging currents involved in US06 driving cycle accelerate the aging process of the onboard battery cell. The percentage of the remaining capacity compared with the 20 Ah nominal capacity is shown in Figure 11. Even though the battery aging process is slower under low temperatures, the original capacity is heavily reduced. Figure 11 and Table 4 show that operating

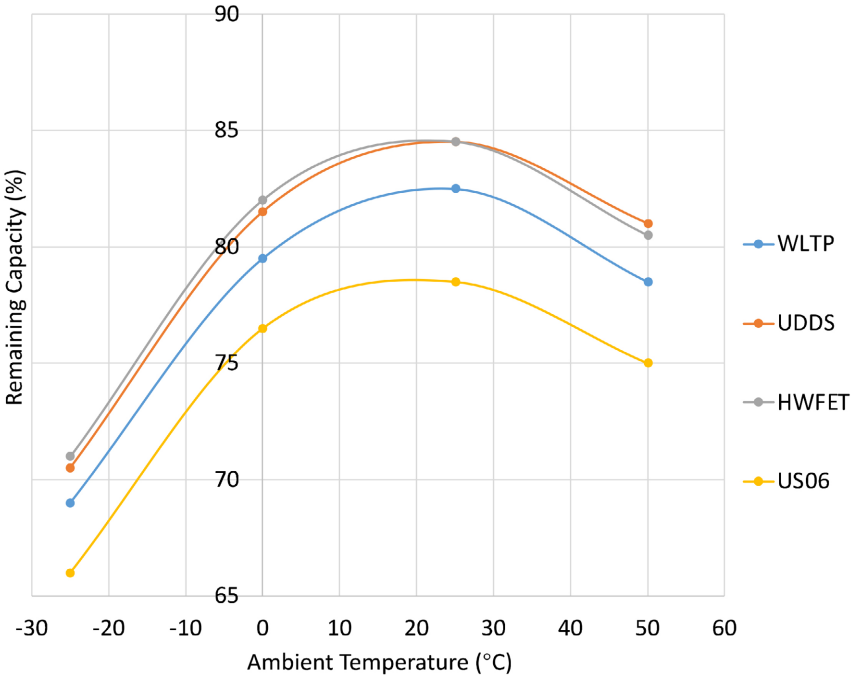

Figure 11. Percentage of remaining capacity of the battery cell compared to nominal capacity after simulated 15,000 hours of different driving cycle repetitions under different ambient temperatures.

Table 4. Effects of different ambient temperatures and different driving cycles on cycle aging of onboard battery cell after 15,000 simulated hours.

	−25 degrees Celsius				0 degree Celsius				25 degrees Celsius				50 degrees Celsius			
	WLTP	UDDS	HWFET	US06	WLTP	UDDS	HWFET	US06	WLTP	UDDS	HWFET	US06	WLTP	UDDS	HWFET	US06
DOD before Recharge	90%															
Original Capacity	16.3 Ah				18.8 Ah				20 Ah				20 Ah			
Capacity after 15,000 h	13.8 Ah	14.1 Ah	14.2 Ah	13.2 Ah	15.9 Ah	16.3 Ah	16.4 Ah	15.3 Ah	16.5 Ah	16.9 Ah	16.9 Ah	15.7 Ah	15.7 Ah	16.2 Ah	16.1 Ah	15 Ah
Capacity Decrement	2.5 Ah	2.2 Ah	2.1 Ah	3.1 Ah	2.9 Ah	2.5 Ah	2.4 Ah	3.5 Ah	3.5 Ah	3.1 Ah	3.1 Ah	4.3 Ah	4.3 Ah	3.8 Ah	3.9 Ah	5 Ah
Remaining Capacity Compared with Nominal Capacity (20 Ah)	69.0%	70.5%	71.0%	66.0%	79.5%	81.5%	82.0%	76.5%	82.5%	84.5%	84.5%	78.5%	78.5%	81.0%	80.5%	75.0%

the electric vehicle under an ambient temperature around 25˚C finds a balance between slower battery aging and larger battery usable capacity. The overall trend of this simulation result is coincident with the published data [24].

The simulation results of the second study on battery cycle aging are presented in Table 5. In this study, the effects of different DOD levels before recharge and different driving cycles on battery cycle aging are investigated. The ambient temperature is set to 25˚C for all simulation cases. Because 25˚C is an optimal ambient temperature for lithium-ion battery, the original capacity is not affected by the ambient temperature. Each driving cycle is repeated until the DOD of the battery cell reaches a preset level, then the battery cell is fully recharged by 10 A current. To investigate the effects of DOD level before each recharge on battery cycle aging, four preset DOD levels are selected for simulations, which are 65%, 75%, 85%, and 95%. Table 5 shows that the capacity decrement after 15,000 hours of usage increases with the DOD level, which means that the cycle aging process of the onboard battery will be accelerated if the battery is almost used up before each recharge every time. The percentage of the remaining capacity compared with 20 Ah nominal capacity is presented in Figure 12. The overall trend of this simulation result is also coincident with the published data [24]. Based on the simulation results of these two studies, to prolong the service life of the onboard battery pack of an electric vehicle, driver should operate the vehicle under an environmental temperature around 25˚C, fully recharge the battery pack at a shallow DOD level, and avoid aggressive driving behaviors.

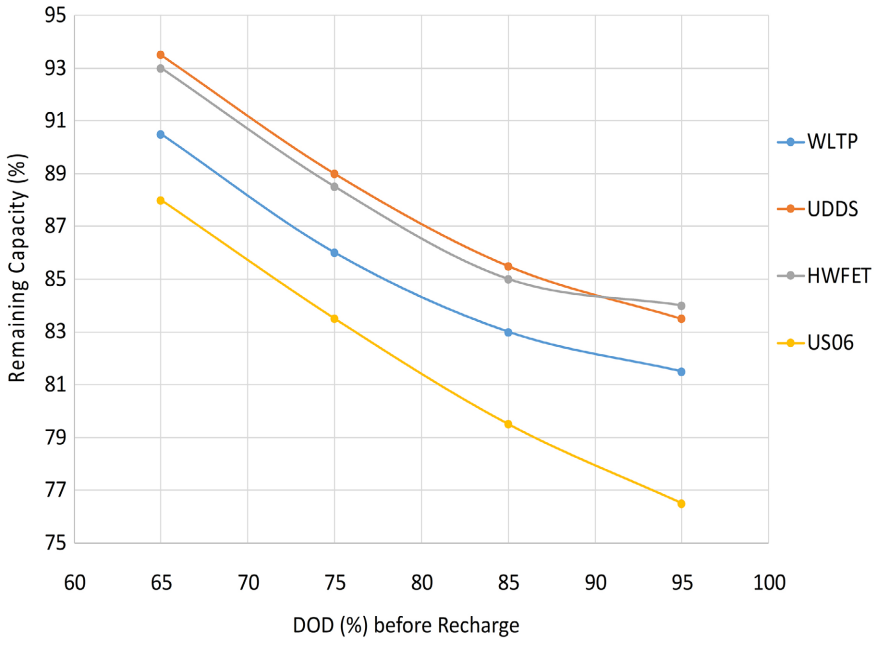

Figure 12. Percentage of remaining capacity of the battery cell compared to nominal capacity after simulated 15,000 hours of different driving cycle repetitions with different DOD levels before each recharge.

Table 5. Effects of different DOD levels before recharge and different driving cycles on cycle aging of onboard battery cell after 15,000 simulated hours.

	65% DOD before Recharge				75% DOD before Recharge				85% DOD before Recharge				95% DOD before Recharge			
	WLTP	UDDS	HWFET	US06	WLTP	UDDS	HWFET	US06	WLTP	UDDS	HWFET	US06	WLTP	UDDS	HWFET	US06
Ambient Temperature	25 Degrees Celsius															
Original Capacity	20 Ah															
Capacity after 15,000 h	18.1 Ah	18.7 Ah	18.6 Ah	17.6 Ah	17.2 Ah	17.8 Ah	17.7 Ah	16.7 Ah	16.6 Ah	17.1 Ah	17.0 Ah	15.9 Ah	16.3 Ah	16.7 Ah	16.8 Ah	15.3 Ah
Capacity Decrement	1.9 Ah	1.3 Ah	1.4 Ah	2.4 Ah	2.8 Ah	2.2 Ah	2.3 Ah	3.3 Ah	3.4 Ah	2.9 Ah	3.0 Ah	4.1 Ah	3.7 Ah	3.3 Ah	3.2 Ah	4.7 Ah
Remaining Capacity Compared with Nominal Capacity (20 Ah)	90.5%	93.5%	93.0%	88.0%	86.0%	89.0%	88.5%	83.5%	83.0%	85.5%	85.0%	79.5%	81.5%	83.5%	84.0%	76.5%

5. Conclusions

In this research, the driving range and battery aging, which are two of the most important topics considered by consumers when purchasing an electric vehicle, are studied. This research started with a series of experiments on the 20 Ah Li-$NiMnCoO_2$ battery cells. Experimental results of discharging voltage, OCV, and internal resistance as functions of DOD are obtained under different ambient temperatures. Effects of cycle aging on battery cell's discharging voltage, OCV, and internal resistance are also investigated by experiments. Experimental results show that low ambient temperature degrades battery cell's performance by lowering its discharging voltage and increasing its internal resistance. Also, about ¼ of the capacity (4.5 Ah out of 18 Ah) of the battery cell is shrunken during an accelerated 800-cycle aging test. The obtained experimental data of the battery cell is used to develop the battery pack model in the electric vehicle model as well as the battery aging model.

The developed electric vehicle model is used to investigate the electric vehicle's driving range. Within the ambient temperature range between −30˚C to 50˚C, the maximum driving range of the electric vehicle decreases with the ambient temperature. Ambient temperatures below 0˚C make the driving range significantly lower. Simulation results show that the maximum driving range of the electric vehicle shrinks by about 30% under −30˚C. The driving range is also heavily affected by driving conditions and driver's driving behaviors. For electric vehicles, urban driving with lower speed and frequent decelerations and stops make the driving range longer, while the driving range of highway driving and aggressive driving with hard accelerations and decelerations is much shorter.

Finally, battery cycle aging of the onboard battery of the electric vehicle after its 15,000-hour usage is investigated. A battery aging model is developed based on the experimental data of the battery cell. The simulated battery cell terminal

currents during electric vehicle driving cycles are used as model input. Simulation results show that, with ambient temperature increases from −25˚C to 50˚C, the shrinkage of usable capacity during 15,000-hour usage becomes larger, which means that the battery cell has a quicker cycle aging process under higher operating temperatures. Battery aging also significantly depends on the driving behaviors of the driver. Large discharging and charging currents involved in aggressive driving can accelerate the aging process of the onboard battery. Simulation results also show that the cycle aging process of the onboard battery will be accelerated if the battery is almost used up before each recharge every time. If the onboard battery is used to 95% DOD every time before recharge, the remaining capacity is only 76.5% to 84% after 15,000-hour usage, depending on which driving cycle was running. Based on the battery aging simulation results, to prolong the service life of the onboard battery pack of an electric vehicle, driver should operate the vehicle under an environmental temperature around 25˚C, fully recharge the battery pack at a shallow DOD level, and avoid aggressive driving behaviors.

In conclusion, this research investigates the driving range and battery aging of electric vehicles in detail and provides quantified results. All developed simulation models are based on first-hand experimental data. This research presents a novel approach to study the driving range and battery aging of electric vehicles and includes valuable results for automotive engineers and consumers of electric vehicles.

Conflicts of Interest

The author declares no conflicts of interest regarding the publication of this paper.

References

[1] Scrosati, B. and Garche, J. (2010) Lithium Batteries: Status, Prospects and Future. *Journal of Power Sources*, **195**, 2419-2430. https://doi.org/10.1016/j.jpowsour.2009.11.048

[2] Ritchie, A. and Howard, W. (2006) Recent Developments and Likely Advances in Lithium-Ion Batteries. *Journal of Power Sources*, **162**, 809-812. https://doi.org/10.1016/j.jpowsour.2005.07.014

[3] Kassem, M., Bernard, J., Revel, R., Pelissier, S., *et al.* (2012) Calendar Aging of a Graphite/LiFePO$_4$ Cell. *Journal of Power Sources*, **208**, 296-305. https://doi.org/10.1016/j.jpowsour.2012.02.068

[4] Bourlot, S., Blanchard, P. and Robert, S. (2011) Investigation of Aging Mechanisms of High Power Li-Ion Cells Used for Hybrid Electric Vehicles. *Journal of Power Sources*, **196**, 6841-6846. https://doi.org/10.1016/j.jpowsour.2010.09.103

[5] Ji, Y., Zhang, Y. and Wang, C.Y. (2013) Li-Ion Cell Operation at Low Temperatures. *Journal of Electrochemical Society*, **160**, 636-649. https://doi.org/10.1149/2.047304jes

[6] Pesaran, A., Santhanagopalan, S. and Kim, G.H. (2013) Addressing the Impact of Temperature Extremes on Large Format Li-Ion Batteries for Vehicle Applications.

Proceedings of the 30*th International Battery Seminar*, Ft. Lauderdale, 11-14 March 2013. https://www.nrel.gov/docs/fy13osti/58145.pdf

[7] Belt, J.R., Ho, C.D., Miller, T.J., Habib, M.A. and Duong, T.Q. (2005) The Effect of Temperature on Capacity and Power in Cycled Lithium Ion Batteries. *Journal of Power Sources*, **142**, 354-360. https://doi.org/10.1016/j.jpowsour.2004.10.029

[8] Fan, J. and Tan, S. (2006) Studies on Charging Lithium-Ion Cells at Low Temperatures. *Journal of the Electrochemical Society*, **153**, 1081-1092. https://doi.org/10.1149/1.2190029

[9] Ping, P., Peng, R., Kong, D., Chen, G. and Wen, J. (2018) Investigation on Thermal Management Performance of PCM-Fin Structure for Li-Ion Battery Module in High-Temperature Environment. *Journal of Energy Conversion and Management*, **176**, 131-146. https://doi.org/10.1016/j.enconman.2018.09.025

[10] Waldmann, T., Wilka, M., Kasper, M., Fleischhammer, M. and Wohlfahrt-Mehrens, M. (2014) Temperature Dependent Ageing Mechanisms in Lithium-Ion Batteries—A Post-Mortem Study. *Journal of Power Sources*, **262**, 129-135. https://doi.org/10.1016/j.jpowsour.2014.03.112

[11] Barre, A., Deguilhem, B., Grolleau, S., Gerard, M., *et al.* (2013) A Review on Lithium-Ion Battery Ageing Mechanisms and Estimations for Automotive Applications. *Journal of Power Sources*, **241**, 680-689. https://doi.org/10.1016/j.jpowsour.2013.05.040

[12] Wright, R., Motloch, C., Belt, J., Christophersen, J., *et al.* (2002) Calendar- and Cycle-Life Studies of Advanced Technology Development Program Generation 1 Lithium-Ion Batteries. *Journal of Power Sources*, **110**, 445-470. https://doi.org/10.1016/S0378-7753(02)00210-0

[13] Ohue, K., Utsunomiya, T., Hatozaki, O. and Yoshimoto, N. (2011) Self-Discharge Behavior of Polyacenic Semiconductor and Graphite Negative Electrodes for Lithium-Ion Batteries. *Journal of Power Sources*, **196**, 3604-3610. https://doi.org/10.1016/j.jpowsour.2010.12.073

[14] Belt, J., Ho, C., Motloch, C., Miller, T., *et al.* (2003) A Capacity and Power Fade Study of Li-Ion Cells during Life Cycle Testing. *Journal of Power Sources*, **123**, 241-246. https://doi.org/10.1016/S0378-7753(03)00537-8

[15] Huang, W., Attia, P.M., Wang, H., Renfrew, S.E., *et al.* (2019) Evolution of the Solid-Electrolyte Interphase on Carbonaceous Anodes Visualized by Atomic-Resolution Cryogenic Electron Microscopy. *Nano Letters*, **19**, 5140-5148. https://doi.org/10.1021/acs.nanolett.9b01515

[16] Guan, P., Liu, L. and Lin, X. (2015) Simulation and Experiment on Solid Electrolyte Interphase (SEI) Morphology Evolution and Lithium-Ion Diffusion. *Journal of the Electrochemical Society*, **162**, A1798-A1808. https://doi.org/10.1149/2.0521509jes

[17] Kotz, R., Ruch, P. and Cericola, D. (2010) Aging and Failure Mode of Electrochemical Double Layer Capacitors during Accelerated Constant Load Tests. *Journal of Power Sources*, **195**, 923-928. https://doi.org/10.1016/j.jpowsour.2009.08.045

[18] Asakura, K., Shimomura, M. and Shodai, T. (2003) Study of Life Evaluation Methods for Li-Ion Batteries for Backup Applications. *Journal of Power Sources*, **119-121**, 902-905. https://doi.org/10.1016/S0378-7753(03)00208-8

[19] Gong, H., Yu, Y., Li, T. and Mei, T. (2012) Solvothermal Synthesis of $LiFePO_4$/C Nanopolyhedrons and Microellipsoids and Their Performance in Lithium-Ion Batteries. *Materials Letters*, **66** 374-376. https://doi.org/10.1016/j.matlet.2011.08.093

[20] Taheri, P. and Bahrami, M. (2012) Temperature Rise in Prismatic Polymer Lithium-Ion Batteries: An Analytic Approach. *The SAE International Journal of Pas-*

senger Cars: *Electronic and Electrical Systems*, **5**, 164-176.
https://doi.org/10.4271/2012-01-0334

[21] Baronti, F., Zamboni, W., Roncella, R., Saletti, R. and Spagnuolo, G. (2015) Open-Circuit Voltage Measurement of Lithium-Iron-Phosphate Batteries. *IEEE International Instrumentation and Measurement Technology Conference* (*I2MTC*) *Proceedings*, Pisa, 11-14 May 2015, 1711-1716.
https://doi.org/10.1109/I2MTC.2015.7151538

[22] Nissan Vehicle Brochures. https://www.nissan.co.uk/vehicles/brochures.html

[23] American Automobile Association (2019) AAA Electric Vehicle Range Testing-AAA Proprietary Research into the Effect of Ambient Temperature and HVAC Use on Driving Range and MPGe. American Automobile Association Inc., Heathrow, 62.

[24] Omar, N., Monem, M., Firouz, Y., Salminen, J., *et al.* (2014) Lithium Iron Phosphate Based Battery—Assessment of the Aging Parameters and Development of Cycle Life Model. *Applied Energy*, **113**, 1575-1585.
https://doi.org/10.1016/j.apenergy.2013.09.003